AIAA SciTech Forum
11–15 & 19–21 January 2021, VIRTUAL EVENT
AIAA Scitech 2021 Forum

10.2514/6.2021-1143

Time and frequency-domain fs/ps CARS measurements and modelling of the CH_4 ν_1 vibrational Q-branch

Timothy Y. Chen[1], Benjamin M. Goldberg[2], Egemen Kolemen[3], Yiguang Ju[4], and Christopher J. Kliewer[5]
[1,3-4]*Department of Mechanical and Aerospace Engineering, Princeton University, Princeton, NJ 08544*
[2,5] *Sandia National Laboratories, Livermore, CA 94550*

Abstract: With the increased interest in CH_4 as a fuel for power generation, propulsion, and catalytic reforming, spatially and time-resolved quantitative measurements of CH_4 are increasingly needed to advance these technologies. Hybrid fs/ps coherent anti-Stokes Raman scattering (fs/ps CARS) has been demonstrated to measure temperature and chemical species concentrations with tens of microns of spatial resolution on the picosecond time scale. However, accurate time-domain and frequency-domain models are necessary to understand the effect of probe delay on the fs/ps CARS signal. In this work, a time-domain model was developed for the CH_4 ν_1 vibrational Q-branch validated by delay scans across pressures ranging from 70 Torr to 600 Torr and furnace set-point temperatures up to 1000 K. A simple modified exponential energy gap (MEG) law was implemented to fit to the room temperature delay scans to approximate the Q-branch linewidths. It was also found that changing the collisional partner did not influence the time-domain decay of the CH_4 Q-branch signal prior to 100 picosecond probe delays. Comparison between simultaneously measured N_2 Q-branch and CH_4Q-branch spectra showed good agreement with evaluated temperatures.

1. Introduction

Hybrid femtosecond/picosecond coherent anti-Stokes Raman scattering (fs/ps CARS) is a laser diagnostic technique that can probe many Raman transitions simultaneously with a broadband femtosecond laser pulse and spatial resolution with tens of microns [1–7]. Non-resonant background associated with four wave mixing is avoided by delaying a spectrally narrow picosecond probe pulse to maintain sufficient frequency resolution. For studies of plasma-assisted flames and catalysis [8–11], it would be beneficial to be able to probe CH_4 with the spatial and temporal resolutions by this ultrafast laser diagnostic technique.

Nanosecond CARS (ns-CARS) has been used to characterize the CH4 ν_1 symmetric stretch Q-branch spectrum with high resolution for many decades [12–15], but only recently has a validated set of Raman frequencies for thermometry been available [16–18]. To our knowledge, this has not yet been adapted for use with fs/ps CARS, although there have been some time-domain ps-CARS measurements performed in an expanding supersonic CH4 jet and a fs/ps CARS time-domain

[1] Ph.D. Candidate, tc8@princeton.edu, Student Member AIAA
[2] Postdoctoral Research Associate, presently at Lawrence Livermore National Laboratory
[3] Assistant Professor
[4] Robert Porter Patterson Professor, Associate Fellow AIAA
[5] Principal Research Scientist

measurements of CH4-N2 mixtures at ambient temperature and pressure [13,19]. Accurate modelling of the fs/ps CARS response in both the frequency and time-domain requires knowledge of both the Raman transition frequencies and the linewidths of each of the transitions [2]. Measurement of the decay of an individual transition can be used to determine its linewidth in the frequency domain and vice-versa. Therefore, the fs/ps CARS signal evolution with increasing probe delay is sensitive to these linewidths, and there is a substantial body of literature dedicated toward measuring these linewidths for rotational and vibrational CARS [20–24]. For CH_4 ns-CARS measurements of the ν_1 Q-branch, semi-classical calculations have typically been used to determine the linewidths [15–17]. However, this approach is complicated and is also dependent on empirical data measured by IR-active modes of CH4 such as the ν_3 mode. Therefore, it would be desirable to develop a simpler linewidth model validated by time-domain CARS measurements of the ν_1 Q-branch. Previous study of the CH_4 ν_1 Q-branch by fs/ps CARS treated the entire peak as one transition and measured its overall linewidth without considering the individual rotational transitions [19]. Treating the peak as a single transition may be a valid assumption at ambient temperature, but at high temperature or long probe delays, the influence of the rotational transitions will appear in the time-domain response. The probe delay scan was also only carried out to 100 ps and at atmospheric pressure. To validate the CH_4 CARS model, a more complete set of validation metrics is needed.

In this study, we use a modified exponential energy gap (MEG) fitting law [25] to approximate the linewidths of the rotational transitions within the ν_1 Q-branch. Such MEG linewidth models have been successfully implemented for the rotational S-branch of O_2 and N_2 [23,24] as well as for the N_2 Q-branch [26]. We use the Raman transition frequencies from [18] calculated by the STDS software [27] and fit probe delay time series scanned up to as long as 1.6 ns. These delay scans were performed at room temperature and pressures ranging from 70 Torr to 500 Torr. Additionally, we use the parameters determined from the MEG model and fit high temperature spectra and delay scans in a tube furnace set to temperatures up to 1000K and pressures from 70 Torr to 600 Torr. With this set of data, we can validate the CH_4 fs/ps CARS model and extend the capabilities of fs/ps CARS to CH_4 quantitative sensing and thermometry.

2. fs/ps CARS Model and Experimental Methods

The theory for calculating fs/ps CARS spectra is outlined in [2] and will not be discussed in detail here. We take an approach similar to [28], to fit the calculated time-domain response of the fs/ps CARS model to the measured delay scans of the probe pulse. In this work, the transition frequencies and intensities from [18] were imported into the CARS code, and subsequently reduced for a given temperature. All Raman frequencies with an intensity below a threshold of 0.3% of the most intense Raman transition as filtered out. This was done to reduce the computational cost to calculate a CARS spectrum, as the original line list contained over 1.7 million transitions. For a rotational temperature of 295 K, the line list was reduced to 336 transitions and contained only Q-branch transitions originating from the vibrational ground state. For a rotational temperature of 1000 K, the line list was reduced to 5900 transitions. Spectra were calculated at time delays equivalent to twice the sampling frequency of the experimental data to minimize computation time while providing sufficient time resolution for fitting. All spectra were calculated on the GPU nodes of the Princeton Adroit research computing cluster. A MEG model was implemented to approximate the linewidths of the transitions within the ν_1 Q-branch using the following expressions [2,25]:

$$\Gamma_{ji} = p\alpha f(T)\left(\frac{T}{T_0}\right)^{-n}\left(1+\frac{a\hbar\omega_{v+1,J_i}/k_BT\delta}{1+a\hbar\omega_{v+1,J_i}/k_BT}\right)^2 \times \exp\left(-\beta\hbar(\omega_{v+1,J_j}-\omega_{v+1,J,i})/\,k_BT\right) \quad (1)$$

$$\Gamma_{ij} = \Gamma_{ji}\frac{2J_i+1}{2J_j+1}\exp\left(\hbar\left(\omega_{v+1,J_j}-\omega_{v+1,J_i}\right)/k_BT\right) \quad (2)$$

$$\Gamma_j = \sum_{i\neq j}\Gamma_{ij} \quad (3)$$

$$f(T) = \frac{1-e^{-m}}{1-e^{-mT/T_0}} \quad (4)$$

where Γ_{ji} is the upward collisional transition from the *i*th rotational state J_i to the *j*th rotational state J_j, Γ_{ij} is the downward collisional transition of the rotational states from J_j to J_i, Γ_j is the linewidth of a transition out of rotational energy level J_j, p is the pressure, T is the temperature, α, β, n, and δ are adjustable parameters in the least-squares fitting, ω_{v+1,J_i} and ω_{v+1,J_j} are the frequency terms representing the rotational energy gap, and f is a temperature dependent function with an additional fitting parameter m. The energy gap is calculated for each rotational energy level by the following expression for rotational energies of spherical top molecules [29]:

$$E_J = BJ(J+1) - DJ^2(J+1)^2 \quad (5)$$

where B and D are the rotational and centrifugal distortion constants of CH_4. For the room temperature spectra calculated in this study, T_0 was set to 295 K, δ =1 and n = 0. Additionally, in the calculations, p and α were combined into a single variable, $p\alpha$. Both simplifications reduce the number of fitting variables down to just $p\alpha$ and β. A spectral library was built using the calculated spectra using a range of $p\alpha$ and β values for the room temperature data. The best fit for β was found by fitting the 300 Torr delay scan, and the other pressures were only fit for $p\alpha$. The high temperature spectra were calculated using the best fit α and β terms to the room temperature measurements. The spectral library was then utilized in a least-squares fit of each of the measured probe delay scans, with α, β, as well as a shift in the time axis as the free variables.

The fs/ps CARS setup is shown in Fig. 1 and is similar to the setup in [3]. The pump/Stokes photons were generated by focusing 1.5 mJ of a Ti:Sapphire regenerative amplifier into a hollow core fiber (Femtolasers). The output of the fiber was a supercontinuum laser pulse with a pulse width of less than 7 fs and 0.6 mJ of total pulse energy. The large bandwidth of the laser pulse made the CH_4 ν_1 Q-branch at 2916 cm^{-1} accessible without a third Stokes beam from an optical parametric amplifier (OPA). A picosecond laser with a pulse width of 65 ps and pulse energy of 3 mJ operating at 20 Hz was used as the probe beam. The oscillator of the picosecond laser was phase locked to the oscillator of the femtosecond laser. The beams were cylindrically focused into sheets and crossed at a 5-degree angle in a 2-beam phase matching configuration. The resulting CARS signal traveled with the probe beam and was separated using an angle-tuned short wave pass filter. The CARS signal was then imaged onto the slit of the spectrometer (Horiba) and detected with a CCD camera (Andor) water-cooled to -80 °C. For the room temperature measurements, the plasma cell from [30] was used with the electrodes removed. For the heated experiments, an 860 mm long quartz tube with a 57 mm inner diameter was placed in a tube furnace (Carbolite) and sealed with O-rings between the tube and the N-BK7 windows. The set point temperatures were 500K, 800K, and 1000K and pressures were varied from 70 Torr to 600 Torr. Gas flows were controlled by mass flow controllers (MKS), and flow rates were set to 500 SCCM. The cell pressure was set by a downstream manual needle valve. The delay between the picosecond laser and the femtosecond laser was controlled electronically (Colby Instruments), and the

maximum delay achievable was limited by the signal-to-noise ratio at the end of the probe delay scan. Delay scans were performed for all measured pressure and temperature conditions.

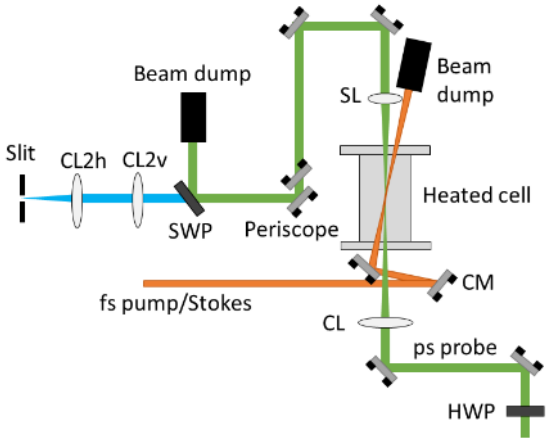

Figure 1. The experimental setup for the heated CARS. CM: plano-concave cylindrical mirror, f =400 mm, CL: plano-convex cylindrical lens, f = 400 mm, SL: plano-convex spherical lens, f = 400 mm, CL2v, CL2h: plano-convex cylindrical lenses, f = 400 mm, 75 mm. HWP: Half-wave plate

3. Results and Discussion

The time delay scans spectrally integrated across the CH_4 ν_1 Q-branch at room temperature were plotted in Fig. 2 as well as the fits. Overall, the coherent beat patterns matched well across all pressures. Additionally, the beat patterns dampened as the pressure increased, which the model also predicted. However, as pressure increased, the fits worsen slightly, particularly in the 100 to 200 ps range for the 500 Torr case. This could be an artifact of approximating the linewidths using a MEG model rather than using a more sophisticated linewidth model. Overall, the fitting was satisfactory, and the α parameter was plotted as a function of pressure as shown in Fig. 3. The fitted α for the lowest pressure case was approximately 20% higher than for the other pressure values. As a result of the variation in α, a linear fit to $p\alpha$ was used as a function of pressure for the high temperature fits. The resultant expression for α is as follows:

$$\alpha = 5.41 \times 10^{-3}\ p^{-1} + 3.85 \times 10^{-4} \quad \textbf{(6)}$$

From Eq. 6, this results in a 1/p (where p is in Torr) dependence for α to reproduce the fitted values. This result was likely because each time delay scan was fit separately and then each best fit was used to determine α.

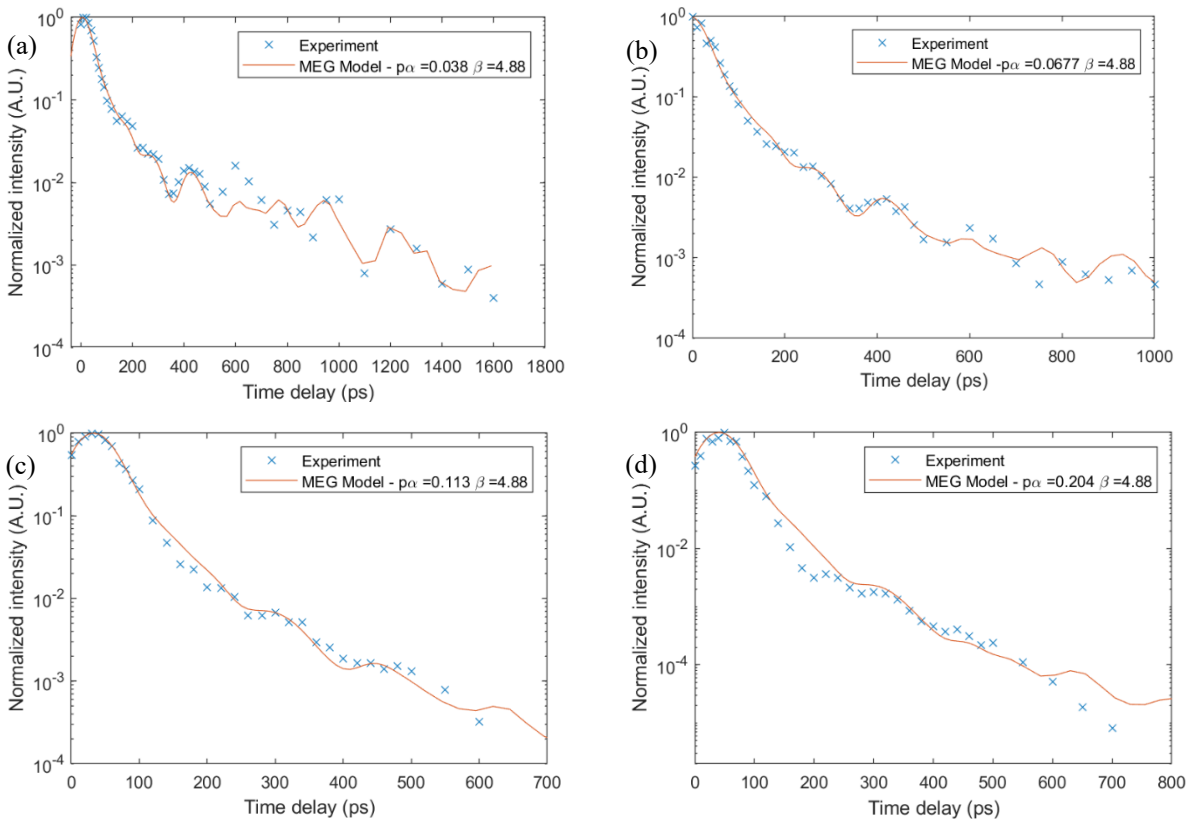

Figure 2. Fitted time delay scans for the CH_4 ν_1 Q-branch for T = 295 K and pressures of 70 Torr (a), 150 Torr (b), 300 Torr (c), and 500 Torr (d).

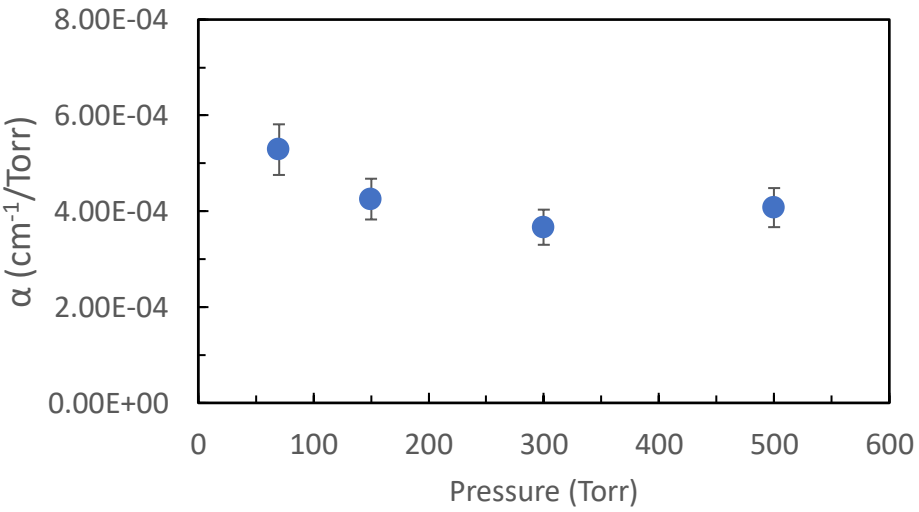

Figure 3. The fitted α after dividing the pα values by their respective pressure.

Next, the effect of exchanging 90% of the pure CH_4 gas mixture at 500 Torr for a different gas was explored. This was to understand how the collisional partner affects the decay rate of the CH_4 Q-branch. As seen in Fig. 4, changing the collisional partner with Ar and N_2 had little effect before

100 ps, marked by the vertical bar. In [19], it was found that varying the CH_4 mole fraction did not modify the measured linewidth. These time delay measurements were carried out up to 100 ps, which was not long enough to see any differences in the time-domain dephasing. However, in the present study, the influence of the mixture composition is evident at longer delays. From Fig. 4, the pure CH_4 mixture has the fastest decay and is followed by N_2 and Ar, respectively.

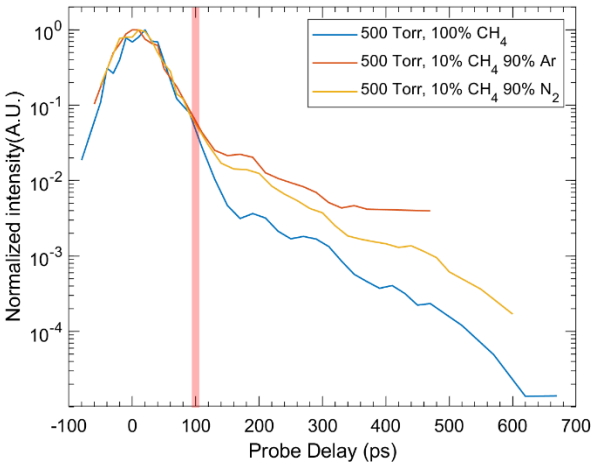

Figure 4. Probe delay scans of pure CH_4, 10% CH_4 – 90% Ar, and 10% CH_4 – 90% N_2 mixtures at 500 Torr, 295 K.

Finally, the potential for performing fs/ps CARS thermometry using CH_4 is demonstrated in Fig. 5. The tube furnace set point was 1000K and the pressure was maintained at 70 Torr. The gas mixture was pure CH_4. Using the linewidth model developed from the room temperature spectra, a spectrum with 30 ps delay was fit in the frequency domain. The early probe delay allowed for frequency-domain fitting without much influence from the time-domain behavior of the CARS signal. The fitted temperature in Fig. 5 was 940 K. The reason for the discrepancy between the tube furnace setpoint and the fitted temperature was most likely due to heat loss from inside the tube furnace to the ambient. The center of the tube furnace, which was specified to be at the setpoint temperature, was located approximately 200 mm downstream from the focus of the CARS beams. This was because a sufficiently long focal length cylindrical mirror was not available to focus the pump/Stokes beam to the center of the furnace. Therefore, at the probed volume, the temperature may not be as high as the setpoint temperature. N_2 vibrational CARS and CH_4 vibrational CARS spectra were measured at each temperature setpoint in 10% CH_4/90% N_2 mixtures at 500 Torr for benchmarking purposes. These spectra were simultaneously acquired by taking advantage of the large bandwidth of the supercontinuum pump/Stokes beam. As seen in Fig. 6, the temperatures determined by the CH_4 Q-branch and N_2 Q-branch spectra are within 17% of each other. Each data point is a temperature evaluated for the CH_4 Q-branch at a different probe delay. At the intermediate temperature, the variance in the two temperatures is the largest, which indicates that further improvements in the time-domain modelling are necessary.

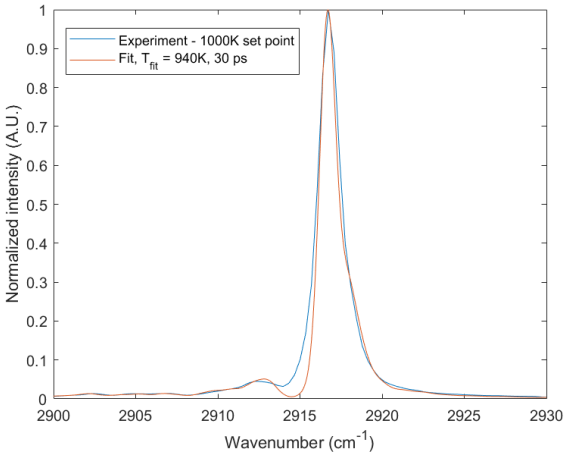

Figure 5. Fitted frequency domain CH_4 spectrum at 70 Torr, tube furnace set point of 1000 K. The fitted temperature was 940 K.

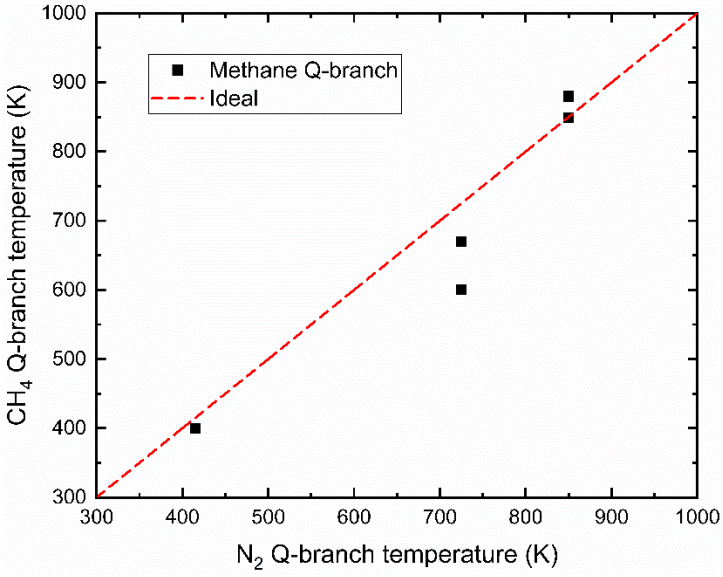

Figure 6. Comparison of CH_4 Q-branch and N_2 Q-branch temperatures evaluated from simultaneously acquired vibrational CARS spectra.

4. Conclusions and Future Work

In this study, a time-domain fs/ps CARS model was developed for the CH_4 ν_1 Q-branch, and thermometry was demonstrated with frequency-domain fitting. It was found that a MEG linewidth model performed satisfactorily for room temperature probe delay scans across a pressure range from 70 to 500 Torr. Previous work demonstrated that the CH_4 ν_1 Q-branch did not vary its time-domain response with changes in CH_4 mole fraction of the mixture. In this study, we showed that the CH_4 Q-branch does not have a significantly different decay rate before 100 picoseconds. However, after this time scale, the mixture effects on the time-domain signal do appear, and measurements made in this regime will need to consider additional collisional effects on the signal. Finally, a CH_4 spectrum measured in a tube furnace, where the fitted temperature was lower than the furnace set-point. It was argued that the measurement location was not at the center of the furnace, so heat loss to the edges of the cell could have caused the mismatch. N_2 vibrational fs/ps

CARS spectra were measured simultaneously with the CH_4 CARS spectra for all temperature set-points to benchmark CH_4 thermometry. The temperature measurements were in good agreement and were within 17% of each other.

Acknowledgements

This material is based upon work supported by the U.S. Department of Energy (DOE), Office of Science, Office of Workforce Development for Teachers and Scientists, Office of Science Graduate Student Research (SCGSR) program. The SCGSR program is administered by the Oak Ridge Institute for Science and Education (ORISE) for the DOE. CJK and BMG were supported by the Office of Chemical Sciences, Geosciences, and Biosciences, Office of Basic Energy Sciences, U.S. Department of Energy. Sandia National Laboratories is a multi-mission laboratory managed and operated by National Technology and Engineering Solutions of Sandia, LLC, a wholly owned subsidiary of Honeywell International, Inc., for the U.S. Department of Energy's National Nuclear Security Administration. YJ would like to thank the funding support of DOE Plasma Science Center, NETL UCFER, and National Science Foundation grants. TYC was partially supported by the Program in Plasma Science and Technology Fellowship (PPST). TYC, EK, and YJ acknowledge the support of ExxonMobil through its membership in the Princeton E-affiliates Partnership of the Andlinger Center for Energy and the Environment. The simulations presented in this article were performed on computational resources managed and supported by the Princeton Institute for Computational Science and Engineering and the Office of Information Technology at Princeton University. We thank Brian D. Patterson for his technical assistance in setting up the furnace experiments.

References

[1] Prince, B. D., Chakraborty, A., Prince, B. M., and Stauffer, H. U. "Development of Simultaneous Frequency- and Time-Resolved Coherent Anti-Stokes Raman Scattering for Ultrafast Detection of Molecular Raman Spectra." *The Journal of Chemical Physics*, Vol. 125, No. 4, 2006, p. 044502. https://doi.org/10.1063/1.2219439.

[2] Stauffer, H. U., Miller, J. D., Slipchenko, M. N., Meyer, T. R., Prince, B. D., Roy, S., and Gord, J. R. "Time- and Frequency-Dependent Model of Time-Resolved Coherent Anti-Stokes Raman Scattering (CARS) with a Picosecond-Duration Probe Pulse." *The Journal of Chemical Physics*, Vol. 140, No. 2, 2014, p. 024316. https://doi.org/10.1063/1.4860475.

[3] Bohlin, A., and Kliewer, C. J. "Two-Beam Ultrabroadband Coherent Anti-Stokes Raman Spectroscopy for High Resolution Gas-Phase Multiplex Imaging." *Applied Physics Letters*, Vol. 104, No. 3, 2014, p. 031107. https://doi.org/10.1063/1.4862980.

[4] Pestov, D., Murawski, R. K., Ariunbold, G. O., Wang, X., Zhi, M., Sokolov, A. V., Sautenkov, V. A., Rostovtsev, Y. V., Dogariu, A., Huang, Y., and Scully, M. O. "Optimizing the Laser-Pulse Configuration for Coherent Raman Spectroscopy." *Science*, Vol. 316, No. 5822, 2007, pp. 265–268. https://doi.org/10.1126/science.1139055.

[5] Dedic, C. E., Meyer, T. R., and Michael, J. B. "Single-Shot Ultrafast Coherent Anti-Stokes Raman Scattering of Vibrational/Rotational Nonequilibrium." *Optica*, Vol. 4, No. 5, 2017, p. 563. https://doi.org/10.1364/OPTICA.4.000563.

[6] Scherman, M., Nafa, M., Schmid, T., Godard, A., Bresson, A., Attal-Tretout, B., and Joubert, P. "Rovibrational Hybrid Fs/Ps CARS Using a Volume Bragg Grating for N_2

Thermometry." *Optics Letters*, Vol. 41, No. 3, 2016, p. 488. https://doi.org/10.1364/OL.41.000488.

[7] Kearney, S. P., and Scoglietti, D. J. "Hybrid Femtosecond/Picosecond Rotational Coherent Anti-Stokes Raman Scattering at Flame Temperatures Using a Second-Harmonic Bandwidth-Compressed Probe." *Optics Letters*, Vol. 38, No. 6, 2013, p. 833. https://doi.org/10.1364/OL.38.000833.

[8] Kameshima, S., Tamura, K., Ishibashi, Y., and Nozaki, T. "Pulsed Dry Methane Reforming in Plasma-Enhanced Catalytic Reaction." *Catalysis Today*, Vol. 256, 2015, pp. 67–75. https://doi.org/10.1016/j.cattod.2015.05.011.

[9] Ju, Y., and Sun, W. "Plasma Assisted Combustion: Dynamics and Chemistry." *Progress in Energy and Combustion Science*, Vol. 48, 2015, pp. 21–83. https://doi.org/10.1016/j.pecs.2014.12.002.

[10] Kim, W., Godfrey Mungal, M., and Cappelli, M. A. "The Role of in Situ Reforming in Plasma Enhanced Ultra Lean Premixed Methane/Air Flames." *Combustion and Flame*, Vol. 157, No. 2, 2010, pp. 374–383. https://doi.org/10.1016/j.combustflame.2009.06.016.

[11] Wang, L., Yi, Y., Wu, C., Guo, H., and Tu, X. "One-Step Reforming of CO_2 and CH_4 into High-Value Liquid Chemicals and Fuels at Room Temperature by Plasma-Driven Catalysis." *Angewandte Chemie International Edition*, Vol. 56, No. 44, 2017, pp. 13679–13683. https://doi.org/10.1002/anie.201707131.

[12] Henesian, M. A., Kulevskii, L., and Byer, R. L. "Cw High Resolution CAR Spectroscopy of the Q (ν_1) Raman Line of Methane." *The Journal of Chemical Physics*, Vol. 65, No. 12, 1976, pp. 5530–5531. https://doi.org/10.1063/1.433015.

[13] Graener, H., Nibler, J. W., and Laubereau, A. "Picosecond Coherent Anti-Stokes Raman Spectroscopy of Molecules in Free Jet Expansions." *Optics Letters*, Vol. 9, No. 5, 1984, p. 165. https://doi.org/10.1364/OL.9.000165.

[14] Kozlov, D. N., Prokhorov, A. M., and Smirnov, V. V. "The Methane N1 (A1) Vibrational State Rotational Structure Obtained from High-Resolution CARS-Spectra of the Q-Branch." *Journal of Molecular Spectroscopy*, Vol. 77, No. 1, 1979, pp. 21–28.

[15] Pieroni, D., Hartmann, J.-M., Chaussard, F., Michaut, X., Gabard, T., Saint-Loup, R., Berger, H., and Champion, J.-P. "Experimental and Theoretical Study of Line Mixing in Methane Spectra. III. The Q Branch of the Raman N1 Band." *The Journal of Chemical Physics*, Vol. 112, No. 3, 2000, pp. 1335–1343. https://doi.org/10.1063/1.480597.

[16] Jourdanneau, E., Chaussard, F., Saint-Loup, R., Gabard, T., and Berger, H. "The Methane Raman Spectrum from 1200 to 5500cm−1: A First Step toward Temperature Diagnostic Using Methane as a Probe Molecule in Combustion Systems." *Journal of Molecular Spectroscopy*, Vol. 233, No. 2, 2005, pp. 219–230. https://doi.org/10.1016/j.jms.2005.07.004.

[17] Jourdanneau, E., Gabard, T., Chaussard, F., Saint-Loup, R., Berger, H., Bertseva, E., and Grisch, F. "CARS Methane Spectra: Experiments and Simulations for Temperature Diagnostic Purposes." *Journal of Molecular Spectroscopy*, Vol. 246, No. 2, 2007, pp. 167–179. https://doi.org/10.1016/j.jms.2007.09.006.

[18] Butterworth, T. D., Amyay, B., Bekerom, D. v. d., Steeg, A. v. d., Minea, T., Gatti, N., Ong, Q., Richard, C., van Kruijsdijk, C., Smits, J. T., van Bavel, A. P., Boudon, V., and van Rooij, G. J. "Quantifying Methane Vibrational and Rotational Temperature with Raman Scattering." *Journal of Quantitative Spectroscopy and Radiative Transfer*, Vol. 236, 2019, p. 106562. https://doi.org/10.1016/j.jqsrt.2019.07.005.

[19] Engel, S. R., Miller, J. D., Dedic, C. E., Seeger, T., Leipertz, A., and Meyer, T. R. "Hybrid Femtosecond/Picosecond Coherent Anti-Stokes Raman Scattering for High-Speed CH_4 /N_2 Measurements in Binary Gas Mixtures: Hybrid Fs/Ps CARS for High-Speed CH_4 /N_2 Measurements." *Journal of Raman Spectroscopy*, Vol. 44, No. 10, 2013, pp. 1336–1343. https://doi.org/10.1002/jrs.4261.

[20] Martinsson, L., Bengtsson, P., Aldén, M., Kröll, S., and Bonamy, J. "A Test of Different Rotational Raman Linewidth Models: Accuracy of Rotational Coherent Anti-Stokes Raman Scattering Thermometry in Nitrogen from 295 to 1850 K." *The Journal of Chemical Physics*, Vol. 99, No. 4, 1993, pp. 2466–2477. https://doi.org/10.1063/1.466197.

[21] Dreier, T., Schiff, G., and Suvernev, A. A. "Collisional Effects in *Q* Branch Coherent Anti-Stokes Raman Spectra of N_2 and O_2 at High Pressure and High Temperature." *The Journal of Chemical Physics*, Vol. 100, No. 9, 1994, pp. 6275–6289. https://doi.org/10.1063/1.467090.

[22] Kulatilaka, W. D., Hsu, P. S., Stauffer, H. U., Gord, J. R., and Roy, S. "Direct Measurement of Rotationally Resolved H2 Q-Branch Raman Coherence Lifetimes Using Time-Resolved Picosecond Coherent Anti-Stokes Raman Scattering." *Applied Physics Letters*, Vol. 97, No. 8, 2010, p. 081112. https://doi.org/10.1063/1.3483871.

[23] Kliewer, C. J., Bohlin, A., Nordström, E., Patterson, B. D., Bengtsson, P.-E., and Settersten, T. B. "Time-Domain Measurements of S-Branch N2–N2 Raman Linewidths Using Picosecond Pure Rotational Coherent Anti-Stokes Raman Spectroscopy." *Applied Physics B*, Vol. 108, No. 2, 2012, pp. 419–426. https://doi.org/10.1007/s00340-012-5037-2.

[24] Miller, J. D., Roy, S., Gord, J. R., and Meyer, T. R. "Communication: Time-Domain Measurement of High-Pressure N2 and O2 Self-Broadened Linewidths Using Hybrid Femtosecond/Picosecond Coherent Anti-Stokes Raman Scattering." *The Journal of Chemical Physics*, Vol. 135, No. 20, 2011, p. 201104. https://doi.org/10.1063/1.3665932.

[25] Koszykowski, M. L., Rahn, L. A., Palmer, R. E., and Coltrin, M. E. "Theoretical and Experimental Studies of High-Resolution Inverse Raman Spectra of Molecular Nitrogen at 1-10 Atm." *The Journal of Physical Chemistry*, Vol. 91, No. 1, 1987, pp. 41–46. https://doi.org/10.1021/j100285a012.

[26] Rahn, L. A., and Palmer, R. E. "Studies of Nitrogen Self-Broadening at High Temperature with Inverse Raman Spectroscopy." *Journal of the Optical Society of America B*, Vol. 3, No. 9, 1986, p. 1164. https://doi.org/10.1364/JOSAB.3.001164.

[27] Wenger, Ch., Boudon, V., Rotger, M., Sanzharov, M., and Champion, J.-P. "XTDS and SPVIEW: Graphical Tools for the Analysis and Simulation of High-Resolution Molecular Spectra." *Journal of Molecular Spectroscopy*, Vol. 251, Nos. 1–2, 2008, pp. 102–113. https://doi.org/10.1016/j.jms.2008.01.011.

[28] Courtney, T. L., and Kliewer, C. J. "Rotational Coherence Beating in Molecular Oxygen: Coupling between Electronic Spin and Nuclear Angular Momenta." *The Journal of Chemical Physics*, Vol. 149, No. 23, 2018, p. 234201. https://doi.org/10.1063/1.5058766.

[29] Tarrago, G., Dang-Nhu, M., and Poussigue, G. "The Ground State of Methane ?H, through the Forbidden Lines of the v3 Band." p. 18.

[30] Chen, T. Y., Goldberg, B. M., Patterson, B. D., Kolemen, E., Ju, Y., and Kliewer, C. J. "1-D Imaging of Rotation-Vibration Non-Equilibrium from Pure Rotational Ultrafast Coherent Anti-Stokes Raman Scattering." *Optics Letters*, 45, 4252-4255 2020.